

A parallel Douglas–Rachford Algorithm for Data on Hadamard Manifolds.

Ronny Bergmann

Technische Universität Chemnitz

Riemannian Geometry in Optimization for Learning,
23rd International Symposium on Mathematical Programming,
Bordeaux, July 2nd, 2018

Manifold-valued Image Processing

Manifold-valued Images

New data acquisition modalities lead to non-Euclidean range

- Interferometric synthetic aperture radar (InSAR)
- Surface normals, GPS data, wind, flow,...
- Diffusion tensors in magnetic resonance imaging (DT-MRI), covariance matrices
- Electron backscattered diffraction (EBSD)



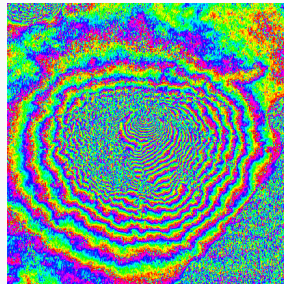
InSAR-Data of Mt. Vesuvius
[Rocca, Prati, Guarneri 1997]

phase-valued data, $\mathcal{M} = \mathbb{S}^1$

Manifold-valued Images

New data acquisition modalities lead to non-Euclidean range

- Interferometric synthetic aperture radar (InSAR)
- Surface normals, GPS data, wind, flow,...
- Diffusion tensors in magnetic resonance imaging (DT-MRI), covariance matrices
- Electron backscattered diffraction (EBSD)



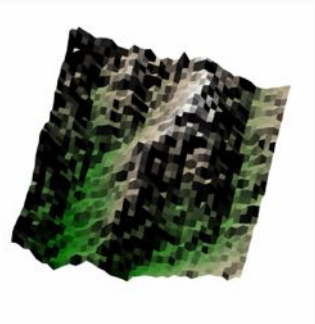
InSAR-Data of Mt. Vesuvius
[Rocca, Prati, Guarneri 1997]

phase-valued data, $\mathcal{M} = \mathbb{S}^1$

Manifold-valued Images

New data acquisition modalities lead to non-Euclidean range

- Interferometric synthetic aperture radar (InSAR)
- Surface normals, GPS data, wind, flow,...
- Diffusion tensors in magnetic resonance imaging (DT-MRI), covariance matrices
- Electron backscattered diffraction (EBSD)

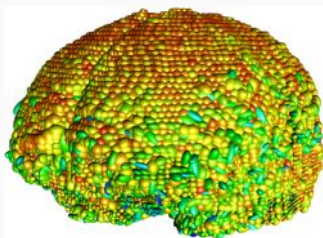


National elevation dataset
[Gesch, Evans, Mauck, 2009]
directional data, $\mathcal{M} = \mathbb{S}^2$

Manifold-valued Images

New data acquisition modalities lead to non-Euclidean range

- Interferometric synthetic aperture radar (InSAR)
- Surface normals, GPS data, wind, flow,...
- Diffusion tensors in magnetic resonance imaging (DT-MRI), covariance matrices
- Electron backscattered diffraction (EBSD)



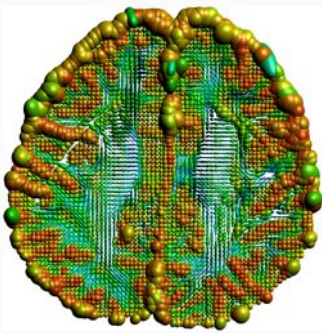
diffusion tensors in human brain
from the Camino dataset
<http://cmic.cs.ucl.ac.uk/camino>

sym. pos. def. matrices, $\mathcal{M} = \text{SPD}(3)$

Manifold-valued Images

New data acquisition modalities lead to non-Euclidean range

- Interferometric synthetic aperture radar (InSAR)
- Surface normals, GPS data, wind, flow,...
- Diffusion tensors in magnetic resonance imaging (DT-MRI), covariance matrices
- Electron backscattered diffraction (EBSD)



horizontal slice #28
from the Camino dataset
<http://cmic.cs.ucl.ac.uk/camino>

sym. pos. def. matrices, $\mathcal{M} = \text{SPD}(3)$

Manifold-valued Images

New data acquisition modalities lead to non-Euclidean range

- Interferometric synthetic aperture radar (InSAR)
- Surface normals, GPS data, wind, flow,...
- Diffusion tensors in magnetic resonance imaging (DT-MRI), covariance matrices
- Electron backscattered diffraction (EBSD)



EBSD example from the MTEX toolbox
[Bachmann, Hielscher, since 2005]

Rotations (mod. symmetry),
 $\mathcal{M} = \text{SO}(3)(/\mathcal{S})$.

Manifold-valued Images

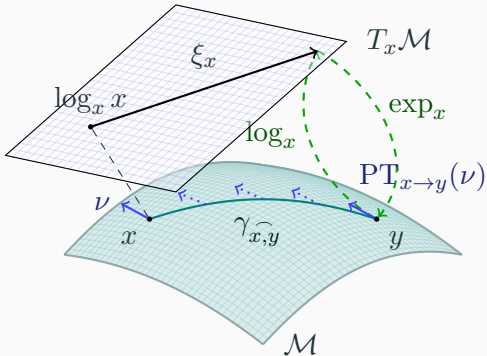
New data acquisition modalities lead to non-Euclidean range

- Interferometric synthetic aperture radar (InSAR)
- Surface normals, GPS data, wind, flow,...
- Diffusion tensors in magnetic resonance imaging (DT-MRI), covariance matrices
- Electron backscattered diffraction (EBSD)

Common properties

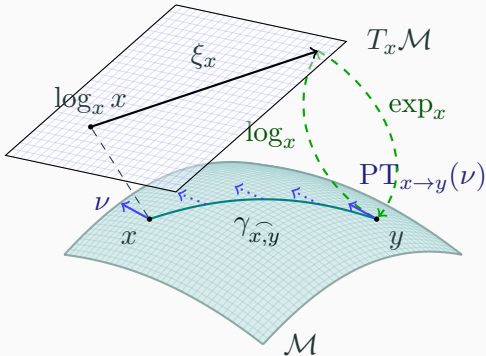
- Range of values is a Riemannian manifold
- Tasks from “classical” image processing

A d -dimensional Riemannian Manifold \mathcal{M}



A d -dimensional Riemannian manifold can be informally defined as a set \mathcal{M} covered with a ‘suitable’ collection of charts, that identify subsets of \mathcal{M} with open subsets of \mathbb{R}^d and a continuously varying inner product on the tangential spaces.

A d -dimensional Riemannian Manifold \mathcal{M}



Geodesic $\gamma_{x,y}$ shortest connection (on \mathcal{M}) between $x, y \in \mathcal{M}$

Tangent space $T_x\mathcal{M}$ at x , with inner product $\langle \cdot, \cdot \rangle_x$

Logarithmic map $\log_x y = \dot{\gamma}_{x,y}(0)$ “speed towards y ”

Exponential map $\exp_x \xi_x = \gamma(1)$, where $\gamma(0) = x$, $\dot{\gamma}(0) = \xi_x$

Parallel transport $\text{PT}_{x \rightarrow y}(\nu)$ of $\nu \in T_x\mathcal{M}$ along $\gamma_{x,y}$

Variational Methods for Euclidean Data

- Let $\mathcal{V} \subseteq \mathcal{G} = \{1, \dots, N\} \times \{1, \dots, M\}$
- **Task:** Given noisy, possibly lossy, data $f: \mathcal{V} \rightarrow \mathbb{R}^m$:
Reconstruct the original image $u_0: \mathcal{G} \rightarrow \mathbb{R}^m$
- **Approach:** Compute minimizer u^* of a **variational model**

$$\mathcal{E}(u) := \begin{array}{ll} \mathcal{D}(u; f) & + \\ \text{data term} & \alpha \mathcal{R}(u), \end{array} \quad \alpha > 0.$$

regularizer/prior

Variational Methods for Euclidean Data

- Let $\mathcal{V} \subseteq \mathcal{G} = \{1, \dots, N\} \times \{1, \dots, M\}$
- **Task:** Given noisy, possibly lossy, data $f: \mathcal{V} \rightarrow \mathbb{R}^m$:
Reconstruct the original image $u_0: \mathcal{G} \rightarrow \mathbb{R}^m$
- **Approach:** Compute minimizer u^* of a **variational model**

$$\mathcal{E}(u) := \begin{array}{c} \mathcal{D}(u; f) \\ \text{data term} \end{array} + \begin{array}{c} \alpha \mathcal{R}(u), \\ \text{regularizer/prior} \end{array} \quad \alpha > 0.$$

- L^2 data term: $D(u; f) = \sum_{i \in \mathcal{V}} \|u_i - f_i\|^2$

Variational Methods for Euclidean Data

- Let $\mathcal{V} \subseteq \mathcal{G} = \{1, \dots, N\} \times \{1, \dots, M\}$
- **Task:** Given noisy, possibly lossy, data $f: \mathcal{V} \rightarrow \mathbb{R}^m$:
Reconstruct the original image $u_0: \mathcal{G} \rightarrow \mathbb{R}^m$
- **Approach:** Compute minimizer u^* of a **variational model**

$$\mathcal{E}(u) := \begin{array}{ll} \mathcal{D}(u; f) & + \\ \text{data term} & \alpha \mathcal{R}(u), \end{array} \quad \alpha > 0.$$

regularizer/prior

- L^2 data term: $D(u; f) = \sum_{i \in \mathcal{V}} \|u_i - f_i\|^2$
- regularizer: Total Variation (**TV**) [Rudin, Osher, Fatemi, 1992]
known to be edge preserving, for example:

$$\text{anisotropic TV: } \mathcal{R}(u) := \sum_{i,j} (\|u_{i+1,j} - u_{i,j}\| + \|u_{i,j+1} - u_{i,j}\|)$$

Variational Methods for Euclidean Data

- Let $\mathcal{V} \subseteq \mathcal{G} = \{1, \dots, N\} \times \{1, \dots, M\}$
- Task:** Given noisy, possibly lossy, data $f: \mathcal{V} \rightarrow \mathbb{R}^m$:
Reconstruct the original image $u_0: \mathcal{G} \rightarrow \mathbb{R}^m$
- Approach:** Compute minimizer u^* of a variational model

$$\mathcal{E}(u) := \begin{array}{ll} \mathcal{D}(u; f) & + \\ \text{data term} & \alpha \mathcal{R}(u), \end{array} \quad \alpha > 0.$$

regularizer/prior

- L^2 data term: $D(u; f) = \sum_{i \in \mathcal{V}} \|u_i - f_i\|^2$
- regularizer: Total Variation (TV) [Rudin, Osher, Fatemi, 1992]
known to be edge preserving, for example:
anisotropic TV: $\mathcal{R}(u) := \sum_{i,j} (\|u_{i+1,j} - u_{i,j}\| + \|u_{i,j+1} - u_{i,j}\|)$
- high dimensional, non-differentiable, convex

Total Variation of Manifold-valued Data

Note. All summands of the ROF model are (squared) distances.

Let $d_{\mathcal{M}}: \mathcal{M} \times \mathcal{M} \rightarrow \mathbb{R}$ denote the geodesic distance on \mathcal{M} .

Then the TV model for **manifold-valued data** $f: \mathcal{V} \rightarrow \mathcal{M}$ reads

$$\mathcal{E}(u) = \sum_{i \in \mathcal{V}} d_{\mathcal{M}}^2(u_i, f_i) + \alpha \sum_{i,j} \left(d_{\mathcal{M}}(u_{i+1,j}, u_{i,j}) + d_{\mathcal{M}}(u_{i,j+1}, u_{i,j}) \right).$$

This can be minimized with

- functional Lifting

[Cremers,Strelakowski, 2011/13; Lellmann, Kötters, Strelakowski, Cremers, 2013]

- Cyclic Proximal Point-Algorithm

[Bačák, 2013; Weinmann, Storath, Demaret, 2014]

- discrete Gradient, Gradient descent, quasi-Newton

[RB, Fitschen, Persch, Steidl, 2017; Celledoni, Eidnes, Owren, Ringholm, 2018;
RB, Chan, Hielscher, Persch, Steidl, 2016]

The Douglas-Rachford Algorithm

Proximum and Reflection

For $\varphi: \mathcal{M}^n \rightarrow (-\infty, +\infty]$ and $\lambda > 0$ the **Proximum** is defined by

[Moreau, 1962; Rockafellar, 1976; Ferreira, Oliveira, 2002]

$$\text{prox}_{\lambda\varphi}(g) := \arg \min_{u \in \mathcal{M}^n} \frac{1}{2} \sum_{i=1}^n d_{\mathcal{M}}(u_i, g_i)^2 + \lambda\varphi(u).$$

! For a minimizer u^* of φ it holds: $\text{prox}_{\lambda\varphi}(u^*) = u^*$.

Proximum and Reflection

For $\varphi: \mathcal{M}^n \rightarrow (-\infty, +\infty]$ and $\lambda > 0$ the **Proximum** is defined by

[Moreau, 1962; Rockafellar, 1976; Ferreira, Oliveira, 2002]

$$\text{prox}_{\lambda\varphi}(g) := \arg \min_{u \in \mathcal{M}^n} \frac{1}{2} \sum_{i=1}^n d_{\mathcal{M}}(u_i, g_i)^2 + \lambda\varphi(u).$$

! For a minimizer u^* of φ it holds: $\text{prox}_{\lambda\varphi}(u^*) = u^*$.

A map \mathcal{R}_p is called **Reflection** on \mathcal{M} , if

$$\mathcal{R}_p(p) = p \quad \text{and} \quad D_p \mathcal{R}_p = -I \quad \text{hold.}$$

Analogous: **Reflection with respect to $\lambda\varphi$**

$$\mathcal{R}_{\lambda\varphi}(x) = \mathcal{R}_{\text{prox}_{\lambda\varphi}(x)}(x)$$

Proximum and Reflection

For $\varphi: \mathcal{M}^n \rightarrow (-\infty, +\infty]$ and $\lambda > 0$ the **Proximum** is defined by

[Moreau, 1962; Rockafellar, 1976; Ferreira, Oliveira, 2002]

$$\text{prox}_{\lambda\varphi}(g) := \arg \min_{u \in \mathcal{M}^n} \frac{1}{2} \sum_{i=1}^n d_{\mathcal{M}}(u_i, g_i)^2 + \lambda\varphi(u).$$

! For a minimizer u^* of φ it holds: $\text{prox}_{\lambda\varphi}(u^*) = u^*$.

A map \mathcal{R}_p is called **Reflection** on \mathcal{M} , if

$$\mathcal{R}_p(p) = p \quad \text{and} \quad D_p \mathcal{R}_p = -I \quad \text{hold.}$$

Analogous: **Reflection with respect to $\lambda\varphi$**

$$\mathcal{R}_{\lambda\varphi}(x) = \mathcal{R}_{\text{prox}_{\lambda\varphi}(x)}(x)$$

Example. On \mathbb{R}^m we have $\mathcal{R}_p(x) = 2p - x = p - (x - p)$.

Proximal Maps for the Summands of the ROF Model

Theorem

[Oliveira, Ferreira, 2002]

For $f \in \mathcal{M}$, $\varphi: \mathcal{M} \rightarrow \mathbb{R}$, $\varphi(x) = d_{\mathcal{M}}^2(x, f)$ and $\lambda > 0$.

the proximal map is given by

$$\text{prox}_{\lambda\varphi}(x) = \gamma_{x,f}^{\frown}\left(\frac{\lambda}{1+\lambda}\right)$$

Theorem

[Weinmann, Storath, Demaret, 2014]

For $\varphi: \mathcal{M} \times \mathcal{M} \rightarrow \mathbb{R}$, $\varphi(x, y) = d_{\mathcal{M}}(x, y)$, $\lambda > 0$, the proximal map is given by

$$\text{prox}_{\lambda\varphi}(x, y) = \begin{cases} \left(\gamma_{x,y}^{\frown}\left(\frac{\lambda}{d_{\mathcal{M}}(x,y)}\right), \gamma_{x,y}^{\frown}\left(1 - \frac{\lambda}{d_{\mathcal{M}}(x,y)}\right)\right) & \text{if } \lambda < \frac{d_{\mathcal{M}}(x,y)}{2}, \\ \left(\gamma_{x,y}^{\frown}\left(\frac{1}{2}\right), \gamma_{x,y}^{\frown}\left(\frac{1}{2}\right)\right) & \text{else.} \end{cases}$$

The Douglas-Rachford Splitting in Euclidean Space

Goal: Minimize

$$\arg \min_{x \in \mathbb{R}^n} \varphi(x) + \psi(x)$$

using a splitting approach

- for linear operators and PDEs [Douglas, Rachford, 1956]
- for monotone inclusion problems [Lions, Mercier, 1979, Eckstein, 1989]
- applications to image processing [Combettes, Pesquet, 2007]

The iteration of the **Douglas-Rachford Algorithm** reads

$$t^{(k+1)} := \frac{1}{2}t^{(k)} + \frac{1}{2}\mathcal{R}_{\lambda\varphi}(\mathcal{R}_{\lambda\psi}(t^{(k)})), \quad k \in \mathbb{N}_0, t^{(0)} \in \mathbb{R}^n,$$

and is related to the minimizer by $x^* = \text{prox}_{\lambda\psi}(\hat{t})$.

The Douglas-Rachford Splitting in Euclidean Space

Goal: Minimize

$$\arg \min_{x \in \mathbb{R}^n} \varphi(x) + \psi(x)$$

using a splitting approach

- for linear operators and PDEs [Douglas, Rachford, 1956]
- for monotone inclusion problems [Lions, Mercier, 1979, Eckstein, 1989]
- applications to image processing [Combettes, Pesquet, 2007]

The iteration of the **Douglas-Rachford Algorithm** reads

$$t^{(k+1)} := \beta t^{(k)} + (1 - \beta) \mathcal{R}_{\lambda\varphi}(\mathcal{R}_{\lambda\psi}(t^{(k)})), \quad k \in \mathbb{N}_0, t^{(0)} \in \mathbb{R}^n, \beta \in (0, 1),$$

and is related to the minimizer by $x^* = \text{prox}_{\lambda\psi}(\hat{t})$.

Hadamard Manifolds and Symmetric Spaces

A manifold \mathcal{H} is called Hadamard manifold, if

$$d_{\mathcal{M}}^2(x, v) + d_{\mathcal{M}}^2(y, w) \leq d_{\mathcal{M}}^2(x, w) + d_{\mathcal{M}}^2(y, v) + 2d_{\mathcal{M}}(x, y)d_{\mathcal{M}}(v, w)$$

holds for all $x, y, v, w \in \mathcal{H}$, i.e. we have a nonpositive sectional curvature. Then

- geodesics $\gamma_{\widehat{x,y}} : [0, 1] \rightarrow \mathcal{H}$ are unique
- $\mathcal{C} \subset \mathcal{H}$ is convex, if $\gamma_{\widehat{x,y}} \subset \mathcal{C}$ for all $x, y \in \mathcal{C}$
- $\varphi : \mathcal{H} \rightarrow (-\infty, \infty]$ is convex on \mathcal{C} if $\varphi \circ \gamma_{\widehat{x,y}}$ is convex
- The reflection reads $\mathcal{R}_p(x) = \exp_p(-\log_p x)$

\mathcal{H} is called symmetric, if \mathcal{R}_p is a isometry for all p .

The Douglas-Rachford Algorithm (DRA)

For $\varphi, \psi \in \Gamma^0(\mathcal{H})$ (proper, convex, lsc.)

Goal: Find minimizer

$$x^* \in \arg \min_{x \in \mathcal{H}} \varphi(x) + \psi(x)$$

Iteration: For some $t^{(0)} \in \mathcal{H}$ compute the
Krasnoselskii-Mann-iteration, $k \in \mathbb{N}_0$,

[RB, Persch, Steidl, 2016]

$$\begin{aligned} s^{(k)} &= \mathcal{R}_{\lambda\varphi}(\mathcal{R}_{\lambda\psi}(t^{(k)})) \\ t^{(k+1)} &= \gamma_{t^{(k)}, s^{(k)}}(\beta_k) \end{aligned}$$

with $\beta_k \in (0, 1)$ and $\sum_{k \in \mathbb{N}} \beta_k(1 - \beta_k) = \infty$

Convergence of the DRA

Theorem

[Kakavandi 2013]

Let $\mathcal{R}_{\lambda\varphi}, \mathcal{R}_{\lambda\psi}$ are nonexpansive and hence $T = \mathcal{R}_{\lambda\varphi} \circ \mathcal{R}_{\lambda\psi}$ is nonexpansive. Let T possess a fix point \hat{t} .

Then the DRA converges for every start point $t^{(0)} \in \mathcal{H}$ to a fix point \hat{t} of T .

Convergence of the DRA

Theorem

[Kakavandi 2013]

Let $\mathcal{R}_{\lambda\varphi}, \mathcal{R}_{\lambda\psi}$ are nonexpansive and hence $T = \mathcal{R}_{\lambda\varphi} \circ \mathcal{R}_{\lambda\psi}$ is nonexpansive. Let T possess a fix point \hat{t} .

Then the DRA converges for every start point $t^{(0)} \in \mathcal{H}$ to a fix point \hat{t} of T .

Theorem

[RB, Persch, Steidl, 2016]

Let $\varphi, \psi \in \Gamma^0(\mathcal{H})$, let there be a minimizer x^* of $\varphi + \psi$, and let $T = \mathcal{R}_{\lambda\varphi} \circ \mathcal{R}_{\lambda\psi}$ be nonexpansive.

Then there exists for every x^* a fix point \hat{t} of T , such that

$$x^* = \text{prox}_{\lambda\psi}(\hat{t})$$

holds. Further, for every \hat{t} , the point $\text{prox}_{\lambda\psi}(\hat{t})$ is a minimizer of $\varphi + \psi$.

Parallelization

Given: $\varphi_i \in \Gamma^0(\mathcal{H}^m)$, $i = 1, \dots, c$

Goal: Find $x^\star \in \arg \min_{x \in \mathcal{H}^m} \sum_{i=1}^c \varphi_i(x)$

Employ: $\Phi(\mathbf{x}) := \sum_{i=1}^c \varphi_i(x_i)$, $\mathbf{x} = (x_1, \dots, x_c)^T \in \mathcal{H}^{mc}$

and $D := \{\mathbf{x} \in \mathcal{H}^{mc} : x_1 = \dots = x_c \in \mathcal{H}^m\} \subset \mathcal{H}^{mc}$

Parallelization

Given: $\varphi_i \in \Gamma^0(\mathcal{H}^m)$, $i = 1, \dots, c$

Goal: Find $x^* \in \arg \min_{x \in \mathcal{H}^m} \sum_{i=1}^c \varphi_i(x) \Leftrightarrow \mathbf{x}^* \in \arg \min_{\mathbf{x} \in \mathcal{H}^{mc}} \Phi(\mathbf{x}) + \iota_D(\mathbf{x})$

Employ: $\Phi(\mathbf{x}) := \sum_{i=1}^c \varphi_i(x_i)$, $\mathbf{x} = (x_1, \dots, x_c)^T \in \mathcal{H}^{mc}$

and $D := \{\mathbf{x} \in \mathcal{H}^{mc} : x_1 = \dots = x_c \in \mathcal{H}^m\} \subset \mathcal{H}^{mc}$

Parallelization

Given: $\varphi_i \in \Gamma^0(\mathcal{H}^m)$, $i = 1, \dots, c$

Goal: Find $x^* \in \arg \min_{x \in \mathcal{H}^m} \sum_{i=1}^c \varphi_i(x) \Leftrightarrow \mathbf{x}^* \in \arg \min_{\mathbf{x} \in \mathcal{H}^{mc}} \Phi(\mathbf{x}) + \iota_D(\mathbf{x})$

Employ: $\Phi(\mathbf{x}) := \sum_{i=1}^c \varphi_i(x_i)$, $\mathbf{x} = (x_1, \dots, x_c)^T \in \mathcal{H}^{mc}$

and $D := \{\mathbf{x} \in \mathcal{H}^{mc} : x_1 = \dots = x_c \in \mathcal{H}^m\} \subset \mathcal{H}^{mc}$

We obtain the parallel Douglas-Rachford algorithm (PDRA):

For a start point $\mathbf{t}^{(0)} \in \mathcal{H}^{mc}$, and $k = 0, \dots$, compute

[RB, Persch, Steidl, 2016]

$$\mathbf{s}^{(k)} = \mathcal{R}_{\lambda\Phi}\mathcal{R}_{\iota_D}(\mathbf{t}^{(k)}),$$

$$\mathbf{t}^{(k+1)} = \gamma_{\mathbf{t}^{(k)}, \mathbf{s}^{(k)}}(\beta_k)$$

$$\Rightarrow x^* = \text{prox}_{\iota_D}(\hat{\mathbf{t}})_1 = \arg \min_{x \in \mathcal{H}^m} \sum_{i=1}^c d_{\mathcal{H}}^2(\hat{t}_k, x) \quad (\text{Fr\'echet mean})$$

Convergence of PDRA for the ROF model

Are the reflections of the ROF model non-expansive?

Convergence of PDRA for the ROF model

Are the reflections of the ROF model non-expansive?

Theorem: Nonexpansiveness of $\mathcal{R}_{\lambda\Phi}$ [RB, Persch, Steidl, 2016]

Let \mathcal{H} be a symmetric Hadamard manifold, $a \in \mathcal{H}$ and $\lambda > 0$.

For $g(x) := d_{\mathcal{H}}^2(a, x)$ and $G(x_0, x_1) := d_{\mathcal{H}}(x_0, x_1)$

the reflections $\mathcal{R}_{\lambda g}$ und $\mathcal{R}_{\lambda G}$ are nonexpansive.

Convergence of PDRA for the ROF model

Are the reflections of the ROF model non-expansive?

Theorem: Nonexpansiveness of $\mathcal{R}_{\lambda\Phi}$ [RB, Persch, Steidl, 2016]

Let \mathcal{H} be a symmetric Hadamard manifold, $a \in \mathcal{H}$ and $\lambda > 0$.

For $g(x) := d_{\mathcal{H}}^2(a, x)$ and $G(x_0, x_1) := d_{\mathcal{H}}(x_0, x_1)$

the reflections $\mathcal{R}_{\lambda g}$ und $\mathcal{R}_{\lambda G}$ are nonexpansive.

Theorem: Nonexpansiveness of \mathcal{R}_{ι_D} [Fernández-León, Nicolae, 2013]

Let \mathcal{H} be a symmetric Hadamard manifold with constant

sectional curvature and \mathcal{C} be a nonempty, convex subset of \mathcal{H} .

Then \mathcal{R}_{ι_C} is nonexpansive.

Convergence of PDRA for the ROF model

Are the reflections of the ROF model non-expansive?

Theorem: Nonexpansiveness of $\mathcal{R}_{\lambda\Phi}$ [RB, Persch, Steidl, 2016]

Let \mathcal{H} be a symmetric Hadamard manifold, $a \in \mathcal{H}$ and $\lambda > 0$.

For $g(x) := d_{\mathcal{H}}^2(a, x)$ and $G(x_0, x_1) := d_{\mathcal{H}}(x_0, x_1)$

the reflections $\mathcal{R}_{\lambda g}$ und $\mathcal{R}_{\lambda G}$ are nonexpansive.

Theorem: Nonexpansiveness of \mathcal{R}_{ι_D} [Fernández-León, Nicolae, 2013]

Let \mathcal{H} be a symmetric Hadamard manifold with constant

sectional curvature and \mathcal{C} be a nonempty, convex subset of \mathcal{H} .

Then \mathcal{R}_{ι_C} is nonexpansive.

⇒ Convergence of PDRA

Numerical Examples

The Manifold-valued Image Restoration Toolbox

- inspired by Manopt¹; focus on image processing
- implemented in Matlab & C++ (`mex`); Julia in preparation
- easy access to manifold-valued image processing
 - Documentation <http://ronnybergmann.net/mvirt/>
 - Code github.com/kellertuer/mvirt/
- manifolds; object with `exp`, `log`, `dist`, `parallelTransport`
 - symmetric positive definite $d \times d$ matrices $\mathcal{P}(d)$
 - special orthogonal group $\text{SO}(3)$
 - spheres \mathbb{S}^n
 - hyperbolic spaces \mathcal{H}^n
 - ...
- algorithms implemented on the abstract `manifold` object
- plot functions and exports to TikZ/Asymptote.

¹manopt.org - Optimization on Manifolds in Matlab

An Algorithm to compare to: CPPA

Decomposing $\mathcal{E} = \sum_{i=1}^c \varphi_i$ we obtain the

Cyclic Proximal Point Algorithmus (CPPA)

[Bertsekas, 2011; Bačák, 2014]

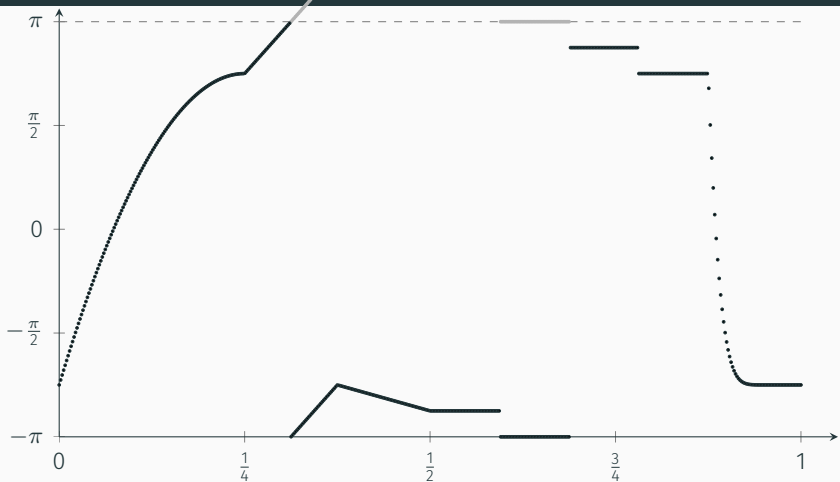
defined for a starting point $x^{(0)} \in \mathcal{M}$ by

$$x^{(k+\frac{i+1}{c})} = \text{prox}_{\lambda_k \varphi_i}(x^{(k+\frac{i}{c})}), \quad i = 0, \dots, c-1, k \geq 0.$$

Convergence of the ROF model

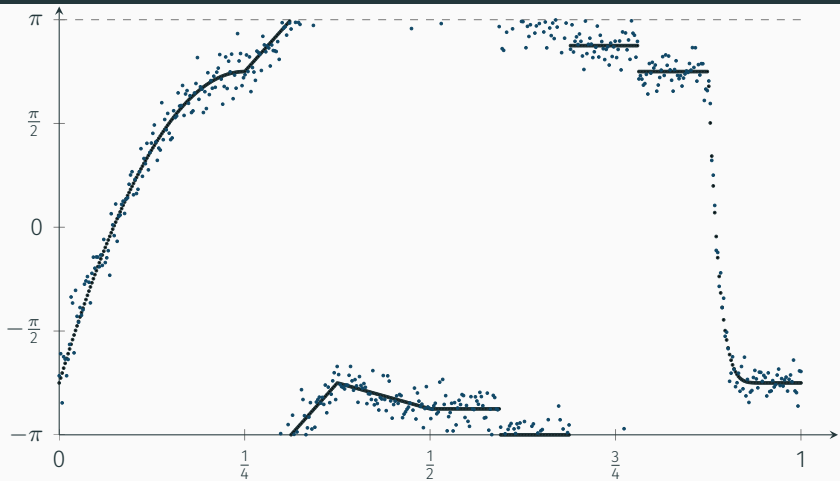
- in Euclidean space $\mathcal{M} = \mathbb{R}^n$ if $\{\lambda_k\}_{k \in \mathbb{N}} \in \ell_2(\mathbb{Z}) \setminus \ell_1(\mathbb{Z})$
- On Hadamard manifolds, if φ_i add. Lipschitz
[Bačák, 2013; Weinmann, Storath, Demaret, 2014]
- with locality restrictions also on \mathbb{S}^1 , $(\mathbb{S}^1)^m \mathbb{R}^n$
[RB, Laus, Weinmann, Steidl, 2014; RB, Weinmann, 2016]
- can be extended to second order differences
[RB, Laus, Weinmann, Steidl, 2014; RB, Weinmann, 2016; Bačák, RB, Weinmann, Steidl, 2016]

A Signal of Cyclic Data



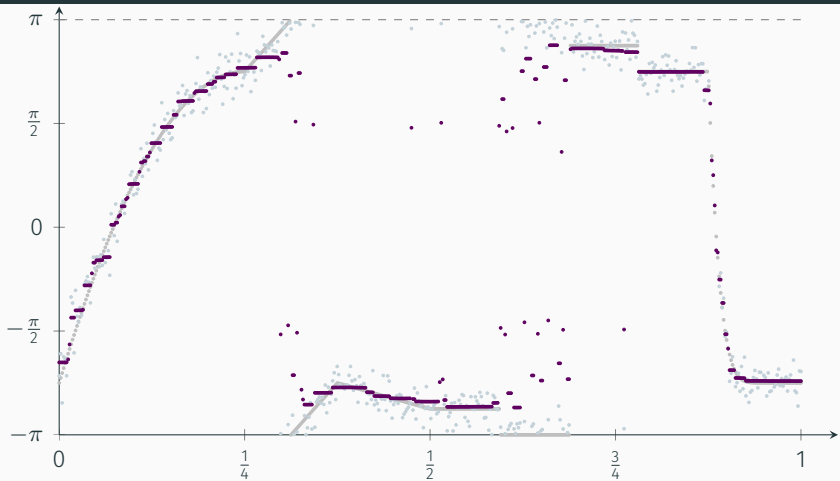
- A function $f: [0, 1] \rightarrow \mathbb{S}^1$ is sampled $\Rightarrow f_0 = (f_{0,i})_{i=1}^{500}$
- Data f stems from the gray plot via modulo
- Jumps $> \pi$ at $\frac{5}{16}$ and $\frac{11}{16}$ just from choice of representation

A Signal of Cyclic Data



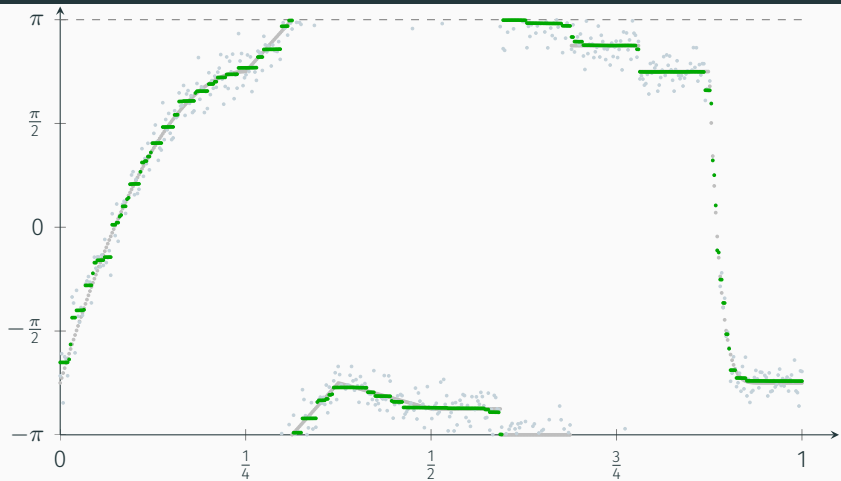
- A function $f: [0, 1] \rightarrow \mathbb{S}^1$ is sampled $\Rightarrow f_0 = (f_{0,i})_{i=1}^{500}$
- Noise: wrapped Gaussian, $\sigma = 0.2$
- noisy $f_n = (f_0 + \eta)_{2\pi}$

A Signal of Cyclic Data



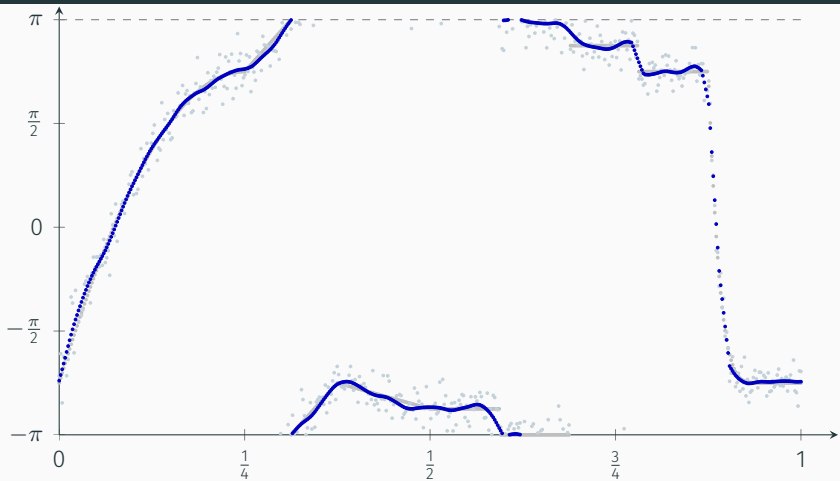
- Comparison of f_0 & f_n width f_R
- Denoised with CPPA and realvalued TV_1 , ($\alpha = \frac{3}{4}$, $\beta = 0$)
- Artefacts at the “jumps that are none“ from representation

A Signal of Cyclic Data



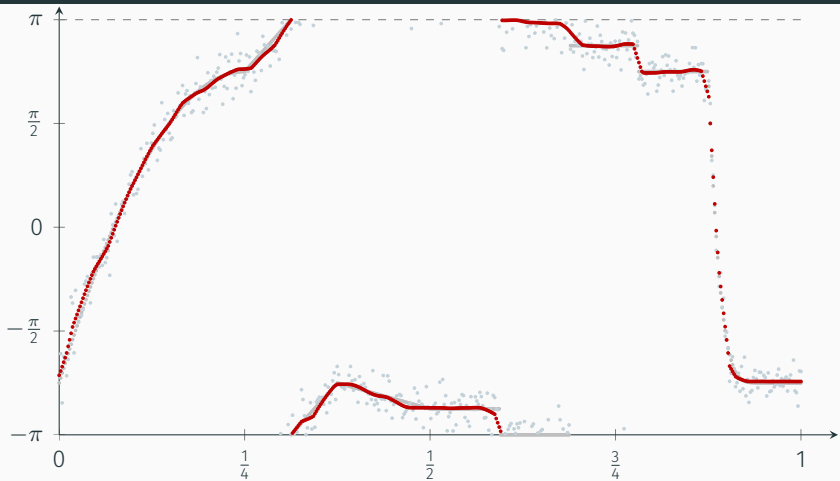
- Comparison of f_0 & f_n width f_1
- Denoised with CPPA and TV_1 ($\alpha = \frac{3}{4}$, $\beta = 0$)
- but: stair caising

A Signal of Cyclic Data



- Comparison of f_0 & f_n width f_2
- Denoised with CPPA and TV_2 ($\alpha = 0, \beta = \frac{3}{2}$)
- but: problems in constant areas

A Signal of Cyclic Data



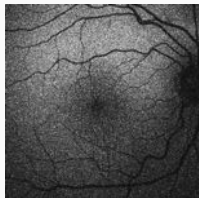
- Comparison of f_0 & f_n width f_3
- Denoised with CPPA and TV_1 & TV_2 ($\alpha = \frac{1}{4}$, $\beta = \frac{3}{4}$)
- combined: smallest mean squared error.

An Image of Gaussian Distributions

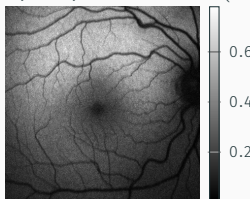
Given: 20 Retina images

[Angulo, Velasco-Forero, 2014]

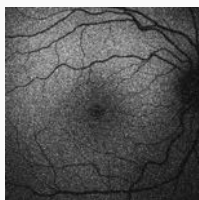
⇒ mean and variance per pixel, $\mathcal{M} = (\mathbb{H}^2)^{384^2}$



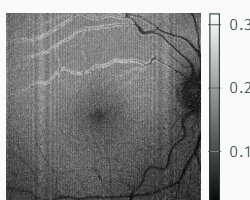
First Image



Measured mean.



Last image.



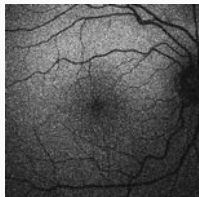
measured variance.

An Image of Gaussian Distributions

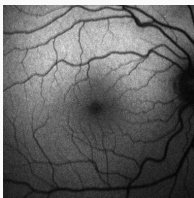
Given: 20 Retina images

⇒ mean and variance per pixel, $\mathcal{M} = (\mathbb{H}^2)^{384^2}$

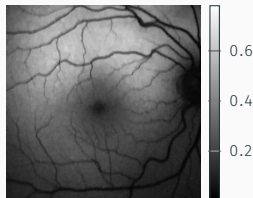
[Angulo, Velasco-Forero, 2014]



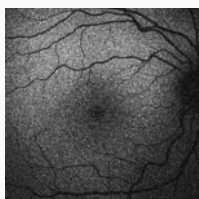
First Image



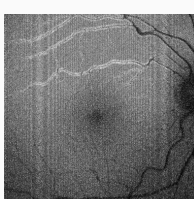
Measured mean.



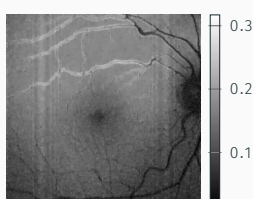
Denoised mean.



Last image.



measured variance.



denoised variance.

Comparison of CPPA & PDRA

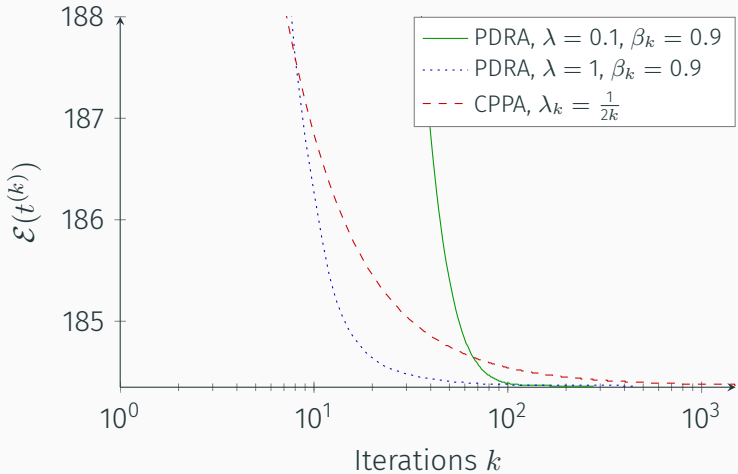
Stopping criterion:

- $\epsilon^{(k)} := \max_{(i,j) \in \mathcal{G}} \left\{ d(t_{i,j}^{(k)}, t_{i,j}^{(k-1)}) \right\} < 10^{-6}$
- $k > 1500$

λ	CPPA in sec.	PDRA		
		$\beta_k = 0.5$	$\beta_k = 0.9$	$\beta_k = 0.95$
0.05	56.85	129.26	65.21	59.84
0.1	56.54	59.21	34.32	36.67
0.5	65.17	57.41	42.06	46.07
1	57.14	93.75	63.58	58.66

Table 1: Runtimes (seconds) of the algorithms.

Comparison of CPPA & PDRA



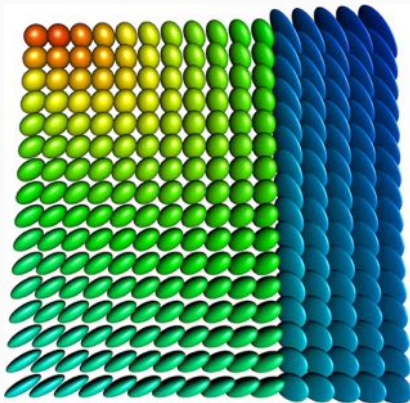
Comparison of CPPA & PDRA

λ	CPPA 184.3643+...	PDRA		
		$\beta_k = 0.5$	$\beta_k = 0.9$	$\beta_k = 0.95$
0.05	44.80	1.021×10^{-5}	1.180×10^{-5}	1.627×10^{-5}
0.1	10.65	2.514×10^{-5}	2.969×10^{-5}	3.429×10^{-5}
0.5	1.055×10^{-2}	5.082×10^{-4}	2.785×10^{-4}	2.256×10^{-4}
1	1.953×10^{-2}	8.189×10^{-4}	5.027×10^{-4}	4.992×10^{-4}

Table 1: Functional values $\mathcal{E}(t^{(k_{\text{last}})})$

Inpainting of a $\mathcal{P}(3)$ -valued Image

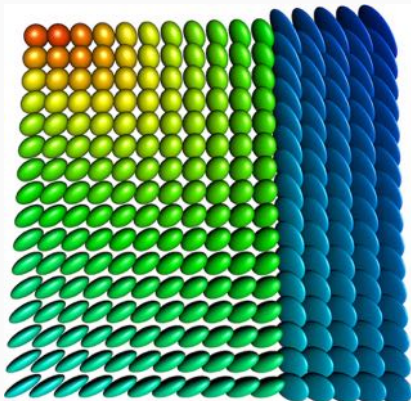
Visualization of sym. pos. def. 3×3 matrices as ellipsoids



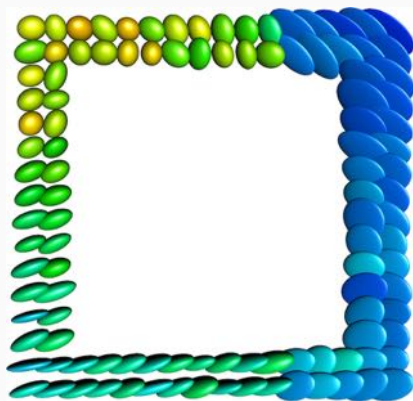
Original.

Inpainting of a $\mathcal{P}(3)$ -valued Image

Visualization of sym. pos. def. 3×3 matrices as ellipsoids



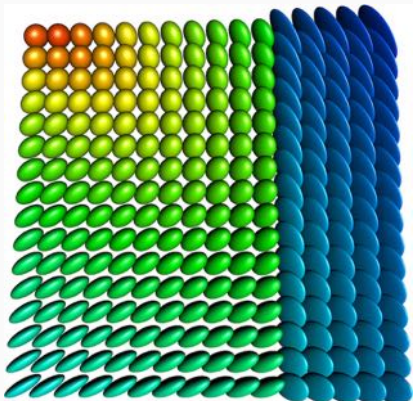
Original.



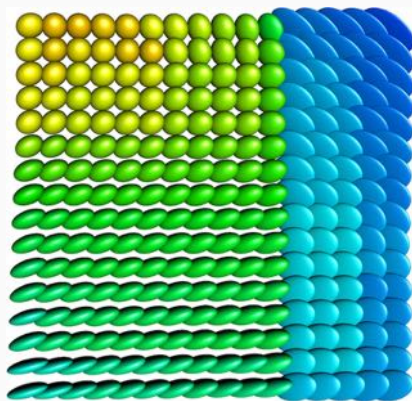
lossy, noisy data

Inpainting of a $\mathcal{P}(3)$ -valued Image

Visualization of sym. pos. def. 3×3 matrices as ellipsoids



Original.



Reconstruction, $\alpha = 0.1$

Conclusion

Conclusion

- Variational methods can be generalized to manifold valued data
- Douglas-Rachford Algorithm for efficient minimization (equiv. to ADMM on \mathbb{R}^n)

Numerical examples implemented in MVIRT

<http://ronnybergmann.net/mvirt/>

which also serves as an easy starting point for manifold-valued image processing. A port to Julia is in progress.

-  RB, J. Persch, and G. Steidl. "A Parallel Douglas–Rachford Algorithm for Minimizing ROF-like Functionals on Images with Values in Symmetric Hadamard Manifolds". In: *SIAM J. Imag. Sci.* 9.3 (2016), pp. 901–937. arXiv: 1512.02814.

 ronnybergmann.net/talks/2018-ISMP18-DouglasRachford.pdf